

Chapter 1

Introduction

1.1 Overview

In the last few decades, we have witnessed some advance and exciting properties in controlling and fabricating nanoelectromechanical (NEMS) and microelectromechanical (MEMS) devices [1, 2, 3]. The development of these types of systems is mainly due to advancements in nanotechnology and its applications. They are useful in detecting highly-sensitive mass [4, 5], spin [6], and charge detectors [7, 8] and help in understanding the basic research related to phonons [9]. Interestingly, NEMS & MEMS open a new window for the experimental understanding of nonlinear dynamics of the discrete system such as nonlinear micromechanical and nanomechanical resonators. In this thesis, we highlighted why nonlinearity is observed in nanoelectromechanical and microelectromechanical systems and study the effect of nonlinear NEMS onto the quantum subsystem. In this chapter we give a basic understanding of NEMS. The use of anharmonic nonlinearity in precise measurement of device and material properties, and also in mass spectrometers [10]. The motion of objects in the macroscopic world has been widely studied over hundreds of years in the field of classical mechanics. Over the last century, quantum mechanics has taken over classical mechanics, and the study of molecular and atomic-scale objects. The boundary

between the two regime classical and quantum is the mesoscopic domain. At which point quantum mechanics took over classical mechanics is studied [11, 12, 13, 14, 15]. Mechanical oscillators are studied in both classical as well as a quantum domain to understand the boundary between them [6, 16, 17, 18]. Recently, the understanding of quantum mechanical phenomena at a large scale by cooling of the mechanical oscillator is achieved. Where the oscillators are cooled up to the ground state [19, 20, 21]. The importance of these devices can be used in the field of quantum computation and quantum metrology. An important question arises why we need to shorten the length of mechanical resonators to reach the nanoscale range. The answer to this is, that one of the most significant regions is its ability to detect small physical quantities and is useful in making sensing devices [5]. In the last few decades the MEMS and NEMS are used in many applications such as for sensing, imaging, and processing applications, including magnetic resonance force microscopy [22] and in RF communications [23]. MEMS have their characteristic length of the order of 100 nm to 1 mm and NEMS has expected length lesser than 100 nm. Fabrication and characterization of experimentally feasible NEMS, used in quantum cavity electrodynamics [24], quantum opto-electromechanics [25] and widely used in the field of quantum computation [26, 27, 28, 29]. It works in an extensive dynamics range. This type of mechanical system is studied for its quantum mechanical behaviour. To achieve the mechanical motion of NEMS in the quantum regime by reducing its size to the nanoscale range, improving its resonant frequency, and cooling the system down to the mK temperatures range [30, 31].

It seems that Nano-electromechanical oscillator operates mainly in the linear regime. But it is harder to maintain NEMS in a linear regime as we know that a small effect of nonlinearity is significant in the nanoscale resonators. The nonlinear nanomechanical oscillator opens a wide range of possibilities for enhancing the performance of NEMS systems. Several experimental studies show nonlinear dynamics of NEMS are useful

in controllable and susceptible devices [2]. The motivation of working in this field is its application in quantum information [32, 33] and testing quantum mechanics on the nanoscale regime of macroscopic objects [34] due to potential nanoscale sensing applications [35, 36]. MEMS are also used as accelerometers in cars to find collisions so that airbags can protect us. It is also used in laptops and mobile phones, so it can turn off the hard drive at fall to prevent damage, and in smartphones, used for the correct orientation of the display [10, 37]. One of the main characteristic features of MEMS and NEMS is Reliability. It is a quantitative measure of the component's strength. It also depends on whether the performance of equipment is satisfactory over time while performing under specified conditions and environment [38]. Over the last few decades, a variety of measures for reliability and techniques were developed [39]. The need for devices made by using MEMS/NEMS is due to their performance and their intended function in the milliseconds to picoseconds range of time. In NEMS, work has been done on a hybrid system in which a quantum system (quantum spin), trapped atoms or ions, or superconducting Josephson junction devices are attached through a magnetic tip to a nanoelectromechanical oscillator [40, 41, 42]. Many types of coupling schemes, and their implementation through experimental demonstrations is already studied [43]. This hybrid NEMS is used in the new approaches to control quantum electromechanical objects, precision sensing, and quantum information processing [44, 45]. This type of system opens interesting perspectives for quantum information technologies and explores the quantum-classical boundary. On the other hand, the motion of resonators helps in making sensitive probes and study the static and dynamic properties of a quantum system. The coupling of the resonator to a two-level system is used to analyze or detect non-classical states. A quantum transducer is used to mediate the interaction between two different quantum systems. Nanomechanical systems combine with such solid-state quantum systems that can be fabricated on chips in such a way that they may interact with spin or charge through

electric or magnetic forces. The dimensions of the system are not limited through optical properties or trapping requirements. The strong interaction between mechanical mode and the two-level system can be achieved more easily without those restrictions. To attain long coherence time in solid-state qubit is more challenging. The solid-state approach to hybrid mechanical systems offers a promising route towards manipulating mechanical motion on a single-phonon level combined with cryogenic temperatures. Techniques for cooling and observing a macroscopic mechanical structure's quantum states of motion are still an open challenge in quantum-state preparation and measurement. On the other hand, superconducting qubits as control and detection elements in NEMS received much attention [46, 47]. Two interesting nonclassical effects have been studied earlier through a linear coupling between a nanomechanical oscillator, and Cooper-pair box system. One is a shift in the energy level of the Cooper-pair through interaction and other is shift in the energy spectrum which depends on fock state of a nanomechanical oscillator [48]. The coupling between the spin qubit and the mechanical motion of the oscillator is already studied [42]. Especially the electronic spin associated with the Nitrogen-Vacancy (NV spin) in diamonds because of its excellent coherence properties. It can be used as a magnetic sensor at the nanoscale range. The study of microscopic two-level systems which have their ground state $|g\rangle$ and excited state $|e\rangle$ and their coupling to the mechanical motion of harmonic oscillator can be found in Refs.[41]. Micromechanical oscillators can be used as an investigator of precision measurements as transducers mediated through photon-phonon interaction. The magnetic tip on Micromechanical oscillators is used as a tool to manipulate spins in quantum systems. The interaction between ultracold atoms and mechanical oscillators is already studied [49]. An experimental study shows the manipulation of the Zeeman state through a micromagnetic cantilever and magnetically trapped Rubidium atoms [50]. The cantilever produces a spatially localized effect that agrees with Landau-Zener's theory [51]. The researchers in this field are trying to achieve a long coherence time due to

coupling between mechanical oscillators and cold atoms [52]. They are mainly interested in studying the dynamics of NV spins that have ample decoherence time and, effectively, spin-1 systems. Such an optomechanical system, coupled through the atom with its internal and external degree of freedom is potentially viable to achieve ground state cooling outside the resolved sideband regime [53, 54] and establishing EPR (Einstein-Podolsky-Rosen) channel [55]. Optical coupling of cold atoms to a mechanical oscillator is used to develop a quantum force sensor that can also beat the standard quantum limit [56]. High-resolution microscopy is the possible application for magnetic coupling of atoms to a resonator. In this thesis we have demonstrated about the coupling of NV center hosted in a diamond nanocrystal with nonlinear nanomechanical oscillators [57]. A recent breakthrough in mass sensing is a device with a mass resolution of 7 zeptograms (7×10^{21}), equivalent to 30 Xenon atoms [5]. Force sensitivity shown by single electron spin detection is remarkably good. In the last few decades, magnetic resonance force microscopy is used in sensing, processing and imaging and shows reforms in RF communications [5]. The reason behind moving to quantum mechanical devices is because decreasing the size of the system will increase its resonance frequency. Also cooling up to Millikelvin range of temperature the mechanical motion of nanoscale resonator will approach to quantum regime [46, 58].

There has been an experimental advancement in characterizing and fabricating NEMS, quantum Opto-electromechanics and cavity quantum electrodynamics giving further understanding in the field of quantum computation as well in understanding quantum hybrid systems [59, 60]. Nano electromechanical hybrid systems are important for quantum information transfer and to get a proper understanding of entanglement and help in the study of quantum-classical boundaries. The characteristic key feature of the NEMS is to obtain high Q factors and low mass, and high frequency in the gigahertz range. Entanglement between two micromechanical resonators are studied recently [61]. Experimentally quantum control has been achieved using the quantum opto-electromechanical protocol

[62]. The quantum nature of mechanical motion can be explored with ground-state cooling is feasible. Furthermore, the coupling between a nanomechanical oscillator and a quantum spin shown in Fig.1.1 was studied [63]. In these types of hybrid systems, there have been various types of qubits realised and proposed. One of them is a NV center, which is a Nitrogen-vacancy defect in a diamond lattice. Mainly, the dynamics of NV center are studied because it has a large decoherence time and is effectively described by a spin-1 system.

Many quantum information applications depend on the way quantum states are distributed either for quantum communication over long distances or within a large computing architecture. In quantum computation qubits and photons are key elements for this purpose [64]. In an atomic system using cavity quantum electrodynamics (QED) light-matter interaction and state transfer protocol has been studied [65]. In the field of solid-state quantum systems, the main challenge is to develop optical interfaces for a broad range of solid-state spin [66] and charge [67, 68] based qubits. The path towards this goal is provided by optomechanics [69], in which a nanomechanical oscillator is coupled with light. This will provide natural setting for an optomechanical transducer (OMT), where indirect coupling between qubit and photon are mediated through the vibration of mechanical device.

1.2 Importance of the study of nonlinearity in NEMS and MEMS

In the last few years, interestingly the nonlinear dynamics of NEMS and MEMS draw attention towards them. Nonlinearity can be easily observed in nano as well as micro-scale mechanical devices [70, 71, 72, 73, 74, 75]. It is important to understand in these devices when nonlinearity is practically needed then exploit it effectively and avoid it when it is

not required. NEMS have opened new experimental territory for understanding nonlinear dynamics. In the recent study nonlinear NEMS are found to have high-frequency range of the order 1 GHz [76, 77, 78]. They work in a relatively weak dissipation regime and with Q factors of the order of 10^2 to 10^4 . An important aspect of this type of system is that steady-state motion as transients tend to disappear before they are detected. For theoretical study purposes, weak dissipation can be considered as a small perturbation. Other than this, one can assemble a large number of coupled resonators that will open new possibilities in the field of nonlinear dynamics for the intermediate degree of freedom that was not possible in macroscopic or in table-top experiments. Coupled-resonator's collective response can be used in the signal enhancement process and noise reduction and many other signal processing applications [79]. For testing discrete nonlinear systems with a large degree of freedom usually array of nanomechanical resonators are studied [80]. Theoretical understanding of these systems may help in future nanotechnology applications.

1.3 Origin of nonlinearity in NEMS resonators

We mainly study mechanical resonators which are performing simple harmonic motion because of linear elastic forces obeying Hooke's law. Hooke's law neglect higher-order terms therefore it shows only linear response. However, in most of the materials the breaking of stress-strain relation leads the system away from linear response. In the equation of motion, the nonlinear effects enter via the force that is proportional to the cubic power of the displacement. This correction will make a simple harmonic oscillator into a duffing oscillator [81]. In this section, we mainly discuss the origin of nonlinear effects with the help of some examples. Nonlinearity is mainly due to the external potential, and some geometric effects that causes it even if the forces involved are linear. The nonlinearity term in duffing oscillator αx^3 , where x is displacement which can be positive or negative. If

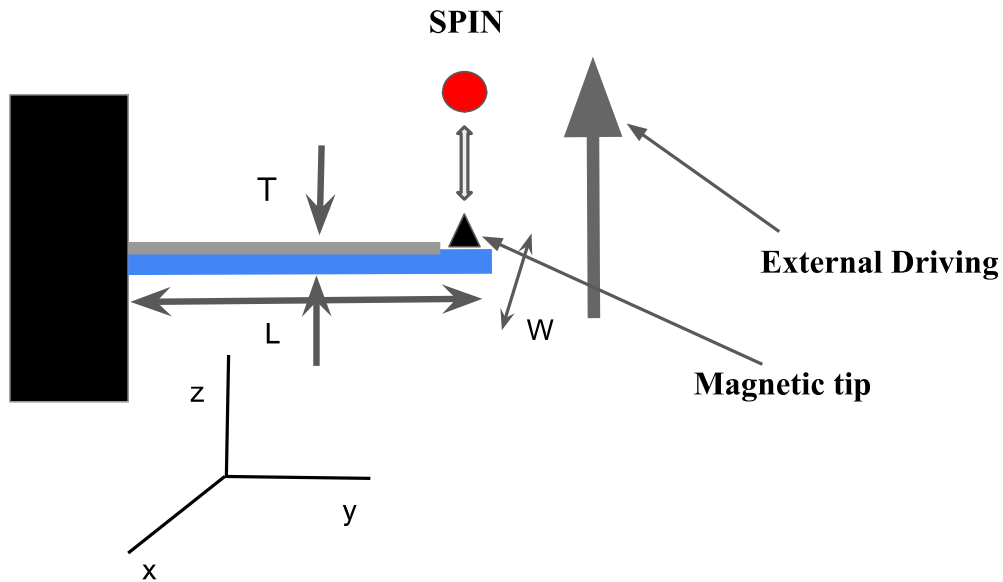


Fig. 1.1 (Color online) Nanomechanical resonator of the dimensions $(L, W, T) = (3000, 300, 30)nm$ attached to a single NV center electron spin with the help of magnetic tip made up of ferromagnetic material at the end of the resonator. The distance between NV center electron spin and magnetic tip is $25nm$ in absence of external driving. Microwave and laser fields are used to manipulate and measure the spin states. Range of Microwave frequency from 100 - 1000 GHz and Nd:YAG laser can be used.

duffing nonlinearity term αx^3 is positive it will assist the linear restoring force increase the resonance frequency and make the oscillator stiffer, while in a negative case it will make the oscillator softer and decrease its resonance frequency. Many experimental analyses of NEMS resonators show nonlinearity due to practical reasons [82]. Actuation and detection mechanisms may include nonlinearities used for interaction with the resonators. Another realization of nonlinearity in NEMS is when the resonator is clamped by its boundaries to its surroundings. These are the external factor that contributes to the nonlinear behaviour of resonators. Finally, nonlinearity often can be found in damping mechanism of every oscillator. We are not going into a detailed description of the damping of a resonator. Whenever we expand the force acting on the resonator up to the cube term of displacement it also consists of a damping term which is proportional to the velocity of the resonator and can also have a nonlinear damping term which is $x^2\dot{x}$ which will increase the amplitude of the oscillation.

1.3.1 Nonlinearity due to external potential and geometry

The effect of external potential on nonlinearity is discussed in some of the previous works such as Cleland and Roukes [7, 8] where they have taken a harmonic oscillator acted by an external electrostatic force. This is done by using oppositely charged NEMS placed near an electrically charged base electrode. Let us consider that in the absence of electric charge, the separation between the resonator and the electrode is d . The deviation from equilibrium position is denoted by x , elastic constant of a spring is k and a constant charge Q is assumed on the resonator. The potential energy of the resonator is given by

$$V(x) = \frac{1}{2}kx^2 - \frac{c}{d+x}, \quad (1.1)$$

where $c = \frac{SQ^2}{4\pi\epsilon_0}$ and S is numerical factor of order unity. To find equilibrium position x_0 in the presence of charge we differentiate Eq. (1.1) with respect to x and get

$$\frac{dV}{dx} = kx + \frac{c}{(d+x)^2} = 0. \quad (1.2)$$

We expand potential acting on the oscillator in a power series of $X = x - x_0$, as

$$\begin{aligned} V(X) &\approx V(x_0) + \frac{1}{2} \left(k - \frac{2c}{(d+x_0)^3} \right) X^2 + \frac{c}{(d+x_0)^4} X^3 - \frac{c}{(d+x_0)^5} X^4 \\ &= V(x_0) + \frac{1}{2} \alpha X^2 + \frac{1}{3} \beta X^3 + \frac{1}{4} \gamma X^4. \end{aligned} \quad (1.3)$$

From the above equation we can write equation of motion as:

$$m\ddot{X} + \alpha X + \beta X^2 + \gamma X^3 = 0, \quad (1.4)$$

where α is the new spring constant, depending on electrostatic attraction to the base electrode, β is a quadratic elastic constant which is positive and will help to drive resonator towards base electrode but independent of the sign of X and γ is duffing constant, m is

mass of oscillator. When $\frac{2c}{(d+x_0)^3} > k$, the restoring force is less than the electrostatic force and the resonator is near the electrode. Let us illustrate how nonlinearities can emerge due to geometric effects from linear forces. The most commonly used NEMS resonator is a doubly-clamped thin elastic beam where both the end of the resonator is clamped making it to deflect only in the transverse direction. If the amplitude of motion is smaller than the width of the resonator then the effect of nonlinearity is negligible. NEMS are quite thin when driven fast and the amplitude can exceed the width. The equation of motion of a thin beam can be derived using the Euler-Bernoulli equation [83]. In equilibrium, the displacement of the resonator in the transverse direction is $Y(z, t)$ which is smaller than the length of the beam is l , and the equation can be written as

$$\rho A \frac{\partial^2 Y}{\partial t^2} = -E \mathcal{I} \frac{\partial^4 Y}{\partial z^4} + T \frac{\partial^2 Y}{\partial z^2}, \quad (1.5)$$

where z is the position along the length of the beam, Y is deflection of an elastic beam normal to its axis and ρ is mass density, A is the area of the cross-section of the beam, E is the Young's modulus, \mathcal{I} is moment of Inertia and T is tension in the beam.

We are going to expand our discussion on NEMS hybrid system which consist of nanomechanical nonlinear resonator and NV center electron spin. We start our discussion with NV center electron spin and further discuss different types of nonlinear nanomechanical oscillators which we used in our study.

1.4 Nitrogen vacancy (NV) center spin

NV center in diamond is a three-level quantum system when two simultaneous excitations can give rise to coherent population trapping. In a three-level system, there will be either two or three transitions making them useful as a light storage device [84].

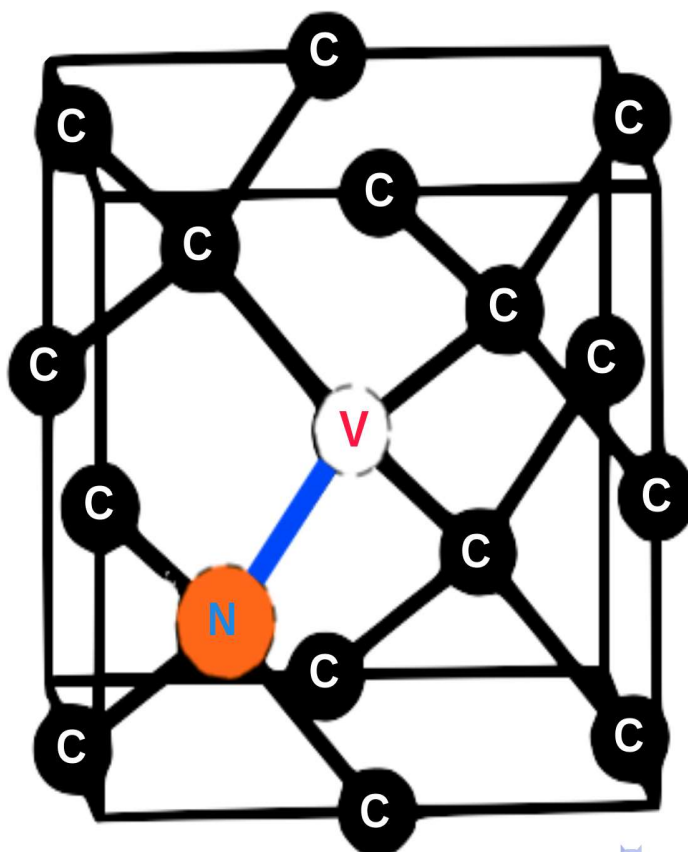


Fig. 1.2 (Color online) Nitrogen vacancy (NV) center in a diamond lattice.

At room temperature in a field-free region, NV centers are point defects in diamonds that possess very long decoherence times. Microwave waves can easily manipulate the NV center's spin. The dynamics of NV center electron spin can be controlled through the external driving that will be useful in making microscopic sensors [6, 85]. NV center electron spins are mainly used in quantum information due to their long coherence time. Loss of coherence is an issue in quantum information, however; many studies have shown the way to minimise it [86, 86]. In the last decade, the effect of the environment on the states were studied widely and various schemes are proposed for the protection of the state by applying fast and strong pulses [87, 88, 89]. Nuclear spins related to NV centers have a larger decoherence time which is upto seconds and thus it can be used in making excellent

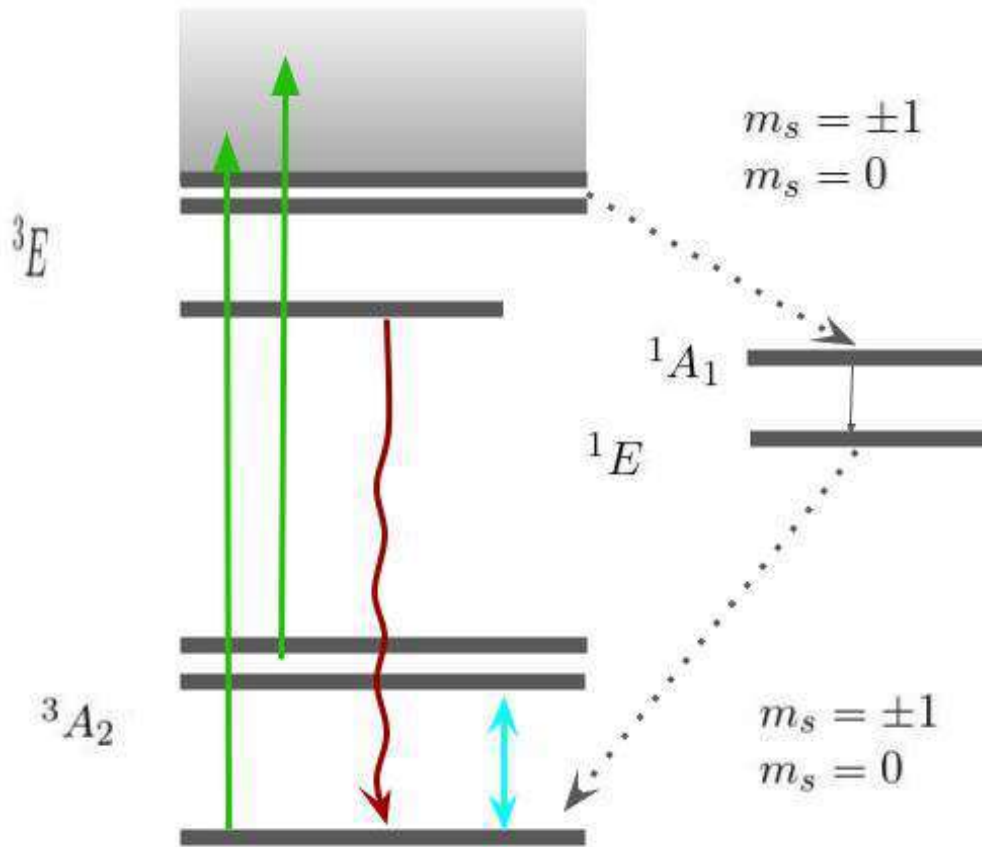


Fig. 1.3 (Color online) Spin dynamics in the NV center in diamond. The transition between ground and excited state is spin conserving. The spin polarization comes from decay via the intermediate singlets state from $m_s = \pm 1$ to $m_s = 0$.

quantum memory devices [90]. Multi-electronic states of the NV center is shown in the Fig.1.3 which is labeled according to their symmetry (E or A) and their spin state triplet (S=1) and for a singlet (S=0). There are two triplet states and two intermediate singlet states. NV center will emit red light when it make transition from 3E to 3A and it will emit green light when it make transition from 3A to 3E .

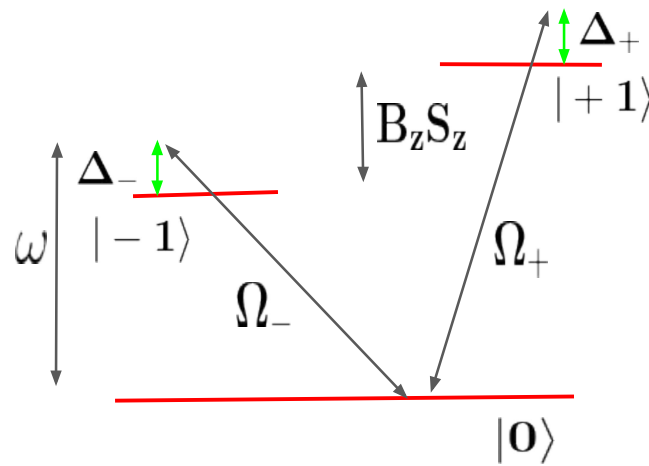


Fig. 1.4 (Color online) Level diagram of the driven NV center in the electronic ground state.

1.4.1 Structure of NV center spin in Diamond

Diamond is a widely known allotrope of carbon possessing sp^3 hybridization and covalent bonds in the form of a tetrahedral geometry. A point defect in a diamond's crystal lattice is created when a carbon atom is replaced by a Nitrogen (N) atom and an adjacent lattice site is left vacant. They are known as the NV center (see Fig.1.2). NV centers are negatively-charged in diamonds and they are a good candidate for solid-state spin qubits. NV center emits red fluorescence signal (600 – 800 nm) when illuminated with green light (532 nm). The system will lead to interfering excitation pathways that depend on the phase of the driving fields and allow for phase control of electromagnetic susceptibilities or coherent population dynamics. These outcomes made three-level systems a cornerstone of quantum optics. Closed-contour interaction(CCI) formed by coherent driving of third available transition gives rise to a new phenomenon, which include phase control coherent population trapping and phase-controlled coherent population dynamics [91].

A novel approach for coherent control of a few level systems has applications in quantum sensing and quantum information processing. NV center electrons are negatively-charged spin-1 ($S=1$) system. The NV center spin consist of three sub-levels ($|m_s\rangle = |0\rangle$ and $|\pm 1\rangle$). In the absence of an external field the spin state $|\pm 1\rangle$ degenerates and shifts from $|0\rangle$ by a zero-field splitting strength $\omega = 2.87GHz$. Microwave field is used for transition between $|0\rangle \rightarrow |\pm 1\rangle$. For weak applied magnetic field $|\mu_B B| \ll \hbar\omega$. The magnetic field will cause Zeeman splitting in the state $|\pm\rangle$. This will lead to a V-type three level system represented in Fig 1.4. Hamiltonian of three-level NV centre in the basis of $|0\rangle, |\pm 1\rangle$ can be written as:

$$\hat{H}_{NV} = \sum_{k=\pm 1} -\hbar\Delta_k |k\rangle\langle k| + \frac{\hbar\Omega_k}{2} (|0\rangle\langle k| + |k\rangle\langle 0|), \quad (1.6)$$

where Δ_k and Ω_k are detuning and Rabi frequency respectively. In this thesis, we mainly use NV centers as qubits. NV centres have many properties that resemble with those of trapped-ion atomic systems. It has a decoherence time of the order of milliseconds which is greater than the superconducting qubits. It can also be manipulated easily with the help of microwaves.

In the next section we going to study about Quantum mechanical oscillators.

1.5 Quantum mechanical oscillators

In the classical mechanics equation of motion which contains nonlinearity, there will be dynamic stochasticity that arises when the repulsion of phase trajectories occurs at a sufficiently quick rate. In quantum case, the system dynamics are described by a wave function, while there is no concept of phase trajectories. The classical-stochastic motion in the quantum analogy is usually known as quantum chaos. It is interesting to choose a parametrically dependent Hamiltonian $H(Q, P, l)$, where Q and P are canonical

coordinates and l is the parameter related to the external field. This type of system is used to study quantum points and other problems of mesoscopic physics [92]. The Hamiltonian $H(Q, P, l)$ of such system for $l = 0$ is exactly integrable. As we increase l , the Hamiltonian becomes nonintegrable and, for a certain value of l_0 , solutions of the classical equations show chaotic behaviour. The parameter l_0 and $l + dl$, where dl is small change in l , is responsible for chaos in the Hamiltonian $H(Q, P, l)$. We have taken the basic Hamiltonian of the quantum pendulum. The Schrödinger equation for the quantum pendulum can be solved using the Mathieu equation. Mathieu-Schrödinger equation under the action of optical pumping in the area of large quantum numbers of the atom is already studied by Zaslavsky and Berman [93]. The behaviour of a quantum pendulum in the field of dynamic stochasticity was studied using quasiclassical approximation [94]. In the case of the classical pendulum stochastic lies near the separatrix [95]. We are going to study about an atom as a nonlinear oscillator under the influence of a variable field. The Hamiltonian can be written in the form:

$$H(x, p, t) = H_0(x, p) + H_{NL} + \varepsilon V(x, t), \quad (1.7)$$

where, $H_0 = \frac{p^2}{2m} + \frac{1}{2} m \omega_0 x^2$ and $H_{NL} = \beta x^3 + \gamma x^4$. The driving term of the oscillator in RF field with frequency ω is given as

$$V(x, t) = V_0 x \cos \omega t, \varepsilon V_0 = f_0, \varepsilon \ll 1. \quad (1.8)$$

Here, the coordinate and momentum of particle is defined by x and p . For simplicity we transform the above Hamiltonian using action-angle variable (I, θ) , with a transformation $x = \sqrt{\frac{2I}{m\omega_0}} \cos \theta$ and $p = -\sqrt{2Im\omega_0} \sin \theta$, resonance condition can be realised at $\omega = \omega_0$ and after averaging over fast phase θ we get transformed Hamiltonian as:

$$H = H_0(I) + \varepsilon V(I) \cos \varphi, \quad (1.9)$$

where, $H_0(I) = \omega_0 I + H_{NL}(I)$. Averaging H_{NL} over fast phase θ gives

$$\begin{aligned} \int \beta x^3 &= \int_0^{2\pi} \beta \left(\frac{2I}{m\omega_0} \right)^{3/2} \cos^3 \theta = 0, \\ \int \gamma x^4 &= \int_0^{2\pi} \gamma \left(\frac{2I}{m\omega_0} \right)^2 \cos^4 \theta = \frac{3\pi}{4} \gamma \left(\frac{2I}{m\omega_0} \right)^2. \end{aligned} \quad (1.10)$$

After substitution we get $H_{NL}(I) = \frac{3\pi}{4} \gamma \left(\frac{2I}{m\omega_0} \right)^2$, $\varphi = \theta - \omega t$, $\varepsilon V(I) = \sqrt{I/m\omega_0} V_0$. The role of frequency can be seen by differentiating H_0 with respect to action (I) which is $\Omega_{NL} = \frac{6\pi I \gamma}{m^2 \omega_0^2}$. The nonlinear resonance condition is fulfilled when $\omega_0 + \Omega_{NL} = \omega$ for action $I = I_0$. For small deviation in action (I) from the resonance value $\Delta I = I - I_0$ ($\Delta I \ll I_0$) after power series expansion [96]. Where ΔI can be transformed in an operator form $\Delta I \rightarrow i \hbar \frac{\partial}{\partial \varphi}$ using corresponding principle.

The Schrödinger equation for any system can be written in the form of:

$$\hat{H} \psi_n = E_n \psi_n \quad (1.11)$$

The Hamiltonian can be written in the form:

$$\hat{H} = -\frac{\hbar^2 \omega'}{2} \frac{\partial^2}{\partial^2 \varphi} + V \cos \varphi, \quad (1.12)$$

where $V(l, \phi) = l \cos \phi$. Schrödinger equation in Mathieu function form is:

$$\frac{\partial^2 \psi_n}{\partial^2 \varphi} + (E_n - V(l, \varphi)) = 0, \quad (1.13)$$

where some dimensionless quantities are introduced such as $E_n \rightarrow \frac{8E_n}{\hbar^2 \omega'}$ and $l \rightarrow \frac{4V}{\hbar^2 \omega'}$, l is strength of pumping. The derivative of non-linear frequency with respect to action is $\omega' = \frac{d\omega(I)}{dI}$. There is specific dependence of barrier height l in Mathieu-Schrödinger equation in the Eigenvalues $E_n(l)$ and eigenvectors $\psi_n(\varphi, l)$. The energy spectrum of Mathieu-Schrödinger equation contain two degenerate domains G_{\pm} and one non-degenerate G_0 .

while the irreducible basis functions for each subgroup are

$$G_- \rightarrow |\phi_n^\pm(\varphi, l)\rangle = \frac{1}{\sqrt{2}}(ce_n(l, \varphi) \pm ise_n(l, \varphi)), \quad (1.14)$$

$$G_0 \rightarrow ce_n(l, \varphi), se_n(l, \varphi), \quad (1.15)$$

and

$$G_+ \rightarrow |\psi_n^\pm(\varphi, l)\rangle = \frac{1}{\sqrt{2}}(ce_n(l, \varphi) \pm ise_{n+1}(l, \varphi)). \quad (1.16)$$

Here, $ce_n(l, \varphi)$ and $se_n(l, \varphi)$ are Mathieu functions with characteristic values $a_n(l)$ and $b_n(l)$, respectively. The trigonometric series representation of Mathieu functions are given as [97]:

$$ce_{2m}(l, \phi) = \sum_{r=0}^{\infty} A_{2r}^{(2m)}(l) \cos(2r\phi), \quad (1.17)$$

$$ce_{2m+1}(l, \phi) = \sum_{r=0}^{\infty} A_{2r+1}^{(2m+1)}(l) \cos((2r+1)\phi), \quad (1.18)$$

$$se_{2m+1}(l, \phi) = \sum_{r=0}^{\infty} B_{2r+1}^{(2m+1)}(l) \sin((2r+1)\phi), \quad (1.19)$$

$$se_{2m+2}(l, \phi) = \sum_{r=0}^{\infty} B_{2r+2}^{(2m+2)}(l) \sin((2r+2)\phi). \quad (1.20)$$

Here the Fourier coefficients $A_{2r}^{(2m)}(l)$, $A_{2r+1}^{(2m+1)}(l)$ and $B_{2r+1}^{(2m+1)}(l)$, $B_{2r+2}^{(2m+2)}(l)$ depend on the quantum number m and the barrier height l . Using a mathematical pendulum state we can analyze mean square fluctuations of the velocity operator. As we go to higher excited states the trembling motion is enhanced. Also observed was a link between the phenomena of trembling motion and the uncertainty relations of non-commutative operators of the system [98]. Schrödinger named the trembling motion “Zitterbewegung” which is solved as a

function of ordinary time that predicted rapid oscillatory motion of elementary particles that obey relativistic wave equation. The mathematical pendulum is the simplest system that can have basic properties of dynamic stochastic. It is also seen that in a mathematical pendulum system the entropy reaches to a high value after reaching the equilibrium point, and remains constant [94, 99].

In the next section we are going to study about kicked rotator which is helpful in analysing chaos in classical mechanics.

1.6 Kicked rotator

In a classical dynamical system we may observe chaotic motion under certain conditions even without any random parameters. We investigate stochasticity mainly in two types of problems: (1) The problem related to the mechanical motion of systems. (2) The problem related to the statistical physics. The difference in the analysis of stochasticity in the classical and quantum cases are: In classical mechanics, we can not distinguish whether the system is driven by time-dependent external force or system is closed and stationary while in quantum case we investigate two types of the problem: first is the evolution of a system in the presence of non-stationary disturbance and in the second case study of the energy spectrum and wave function in the stationary case. Classical mechanics does not deal with these second type of problem. We can see Hamiltonian systems as carriers of chaos. If we apply minimal restrictions, we can see some regions in the phase space of a dynamical Hamiltonian showing a mixing of trajectories. A system with N degrees of freedom can be written by using N pairs of generalised coordinates q_j and generalised

momenta p_j (where j is from 1 to N). The Hamiltonian equation of motion is

$$\begin{aligned}\dot{p}_j &= -\frac{\partial H}{\partial q_j}, \\ \dot{q}_j &= \frac{\partial H}{\partial p_j};\end{aligned}\tag{1.21}$$

where the Hamiltonian of the system is a function of generalised momenta p_j and generalised coordinates q_j ,

$$H(p_j, q_j) = H(p_1, p_2, p_3, \dots, q_1, q_2, q_3, \dots).\tag{1.22}$$

In time dependent case we will only consider periodic time driving of an Hamiltonian with time period

$$T = \frac{2\pi}{\omega}.\tag{1.23}$$

i.e., if $H = H(p_j, q_j, t)$ then,

$$H(p_j, q_j, t + T) = H(p_j, q_j, t).\tag{1.24}$$

Here, the time variable is an additional canonical variable so the system is said to have $N + \frac{1}{2}$ degrees of freedom. Chaotic dynamics occur when the system has $\frac{3}{2}$ degree of freedom. The trajectory can be seen in two-dimensional phase plane having points $(p(t_n), q(t_n))$ corresponding to time $t_n = t_0 + nT$. This is also known as Poincare's map. It can be represented as

$$(p_{n+1}, q_{n+1}) = \hat{\mathcal{T}}(p_n, q_n),\tag{1.25}$$

where $\hat{\mathcal{T}}$ is the shift operator by time T . In many physical problems, the Chirikov-Taylor map also known as the standard map is used. The Hamiltonian of a system can be expressed

using a standard map as

$$H = H_0(I) + \varepsilon V(\theta) T \sum_{n=-\infty}^{n=\infty} \delta(t - nT); \quad (1.26)$$

where I and θ are action and angle variables. The unperturbed part of the Hamiltonian is

$$H_0 = H_0(I). \quad (1.27)$$

The perturbed part of the Hamiltonian is driven by a periodic sequence of kicks having time period $T = \frac{2\pi}{\omega}$. Eq. (1.27) represent motion of a free particle, where $I = p$ and $\theta = x$. For a free rotator, θ will take value from $[0, 2\pi]$. We can transform kicks into cosine function using identity

$$\sum_{n=-\infty}^{n=\infty} \delta\left(\frac{t}{T} - n\right) = \sum_{n=-\infty}^{n=\infty} \cos\left(2n\pi \frac{t}{T}\right). \quad (1.28)$$

Now, Eq. (1.26) can be written as:

$$H = H_0(I) + \varepsilon V(\theta) T \sum_{l=-\infty}^{l=\infty} \cos(l\omega t). \quad (1.29)$$

From the above transformed Hamiltonian the equation of motion can be written as:

$$\dot{I} = -\frac{\partial H}{\partial \theta} = -\varepsilon T \frac{\partial V}{\partial \theta} \sum_{n=0}^{n=\infty} \delta(t - nT), \quad (1.30)$$

$$\dot{\theta} = \frac{\partial H}{\partial I} = \frac{dH_0}{dI} = \omega(I). \quad (1.31)$$

Between any two delta kicks I is constant and θ is linear with t . At each kick after doing integration we get I that will change by $-\varepsilon T \frac{\partial V}{\partial \theta}$. If we assume that I_n, θ_n is action and angle at n^{th} and at $n + 1^{\text{th}}$ kicks, action and angle are I_{n+1} and θ_{n+1} . The relation between

(I_{n+1}, θ_{n+1}) and (I_n, θ_n) can be written as:

$$I_{n+1} = I_n - \varepsilon T \frac{\partial V(\theta_n)}{\partial \theta_n} = I_0 f(\theta), \quad (1.32)$$

$$\theta_{n+1} = \theta_n + T \omega(I_{n+1}). \quad (1.33)$$

For convenience we can take

$$T \frac{\partial V(\theta_n)}{\partial \theta_n} = I_0 f(\theta), \quad (1.34)$$

where I_0 takes dimension of action, and $f(\theta)$ is phase $|f(\theta)| \leq 1$.

Change in action using Eq. (1.32) can be written in the form:

$$\Delta I = -\varepsilon I_0 f(\theta). \quad (1.35)$$

As we can see from Eq. (1.35) action is a slowly changing variable, we can write the phase as:

$$K = \left| \frac{\delta \theta_{n+1}}{\delta \theta_n} - 1 \right| = \varepsilon I_0 T \left| \frac{d\omega}{dI} \right| |f'(\theta)|, \quad (1.36)$$

or

$$K = \varepsilon \alpha \omega T |f'(\theta)|. \quad (1.37)$$

Here, α is a dimensionless non-linearity parameter,

$$\alpha = \left| \frac{d\omega}{dI} \right| \frac{I_0}{\omega}. \quad (1.38)$$

Eq. (1.37) represent criterion for stochasticity. The boundary of stochasticity is determined by the condition $K \geq 1$. From Fig. 1.5 we can see that when the criteria of stochasticity

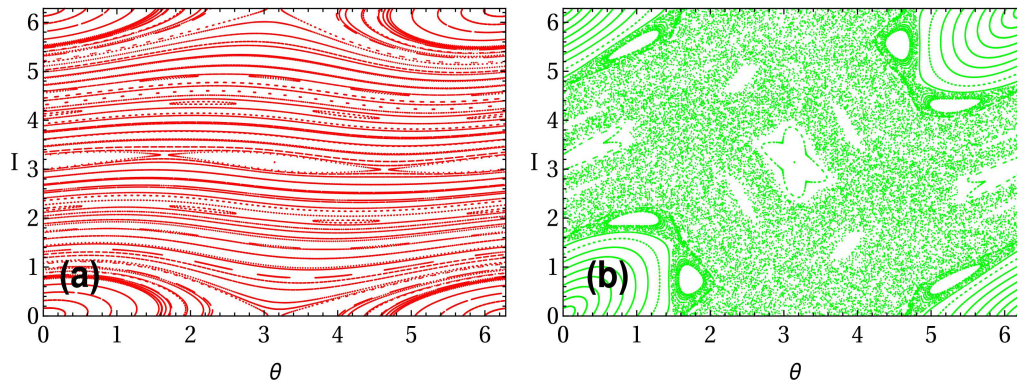


Fig. 1.5 The Phase space plot of Kicked rotator in (a) the regular regime $K = 0.3$ (Red) where the phase space is covered by two different phase trajectories: open hyperbolic and some part of closed elliptic, and (b) the chaotic regime at $K = 1.5$ (Green) where the entire phase space is covered by a chaotic sea.

$K < 1$, the motion of the kicked rotator is in regular regime and we get different type of phase space such as ellipse and open hyperbola. In $K > 1$ case motion of kicked rotator is chaotic the phase space starts merging.

In the next section we are going to expand our discussion about two coupled nonlinear resonators.

1.7 Two coupled nanomechanical resonators

In this section, we develop a qualitative understanding of a complex behaviour of the coupled nonlinear nanomechanical system [100, 101]. There are many efforts being made by experimentalist for fabricating a nanoscale resonators with a precise control of their behavior. Nanoscale resonators are prototype system for testing some fundamental physical phenomenon, such as entanglement and quantum correlations [102]. This will open new approaches to both fundamental physics and technological applications. It shows that the linear and nonlinear response of one oscillator can be modified with the help of driving the second oscillator.

1.7.1 Experimental Setup of coupled nanomechanical resonators

Experimental setup of two strongly coupled nanomechanical resonators, as shown in Fig. 1.6 is taken from [103] using a structure of doubly clamped beams with a shared mechanical ledge. There are three layers of gallium arsenide (GaAs) in which one is 100 nm size and highly n-doped layer and one is an insulating layer of 50 nm and the third one is also of 30nm but p-type doped. In some cases, piezoelectric semiconductors are used to make NEMS resonators. Piezoelectricity, a way to convert mechanical energy into electrical energy in certain types of crystals, has been used in numerous applications ever since it was discovered by the Curie brothers in 1880. Some of the uses of the piezoelectric crystals are in clocks, electrical oscillators and micro-balance. The MEMS with piezoelectricity have their active layers thickness of the order of μm that helps them in gaining strong electromechanical coupling. The nanoscale devices particularly cantilever and beam flexural-mode resonators are used in single-molecule mass sensors and single-cell-level force sensors [5, 104].

1.7.2 Theoretical Modeling of coupled nanomechanical resonators

Dynamics of the system of two strongly interacting nonlinear resonators can be see through a coupled equations of motion in fundamental modes (x_1, x_2) as

$$\ddot{x}_1 + \eta_1 \dot{x}_1 + \omega_1^2 x_1 + \beta_1 x_1^3 + D(x_1 - x_2) = F_1 \cos \Omega_1 t, \quad (1.39)$$

$$\ddot{x}_2 + \eta_2 \dot{x}_2 + \omega_2^2 x_2 + \beta_2 x_2^3 + D(x_2 - x_1) = F_2 \cos \Omega_2 t; \quad (1.40)$$

where F , Ω are the amplitude and frequency of the external driving, D is linear coupling coefficient, $\omega_{1,2}$ are frequencies of the individual resonators, $\eta_{1,2}$, $\beta_{1,2}$ are damping and nonlinearity constants [100]. Right-hand side terms represent the external drives applied

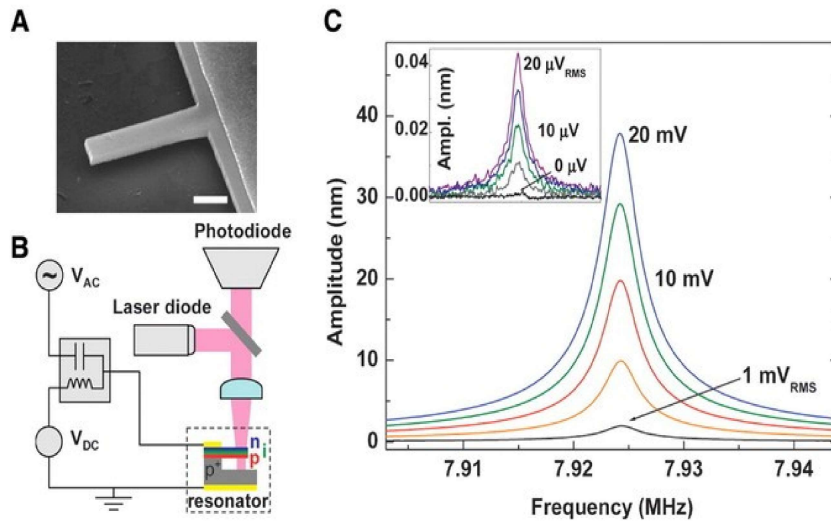


Fig. 1.6 The figure is taken from Sotiris C. Masmanidis et al. science.1144793 (2007) only to depict a case of Nanomechanical piezoelectric actuation. (A) Shows a GaAs cantilever with embedded pin diode structure. (B) Setup for measurement used by Masmanidis et al. The bias T allows both dc and ac signals to be applied. The measurement are performed by Masmanidis et al. at room temperature and a pressure of 5 millitorrs. (C) Frequency response curve near the resonance of a diode-embedded cantilever under 0 dc bias.

to the two oscillators which are controlled independently. If we ignore linear terms in the above equation, we will get two modes of frequency one from the driving term and the second from dissipation and the corresponding eigenvectors are χ_I, χ_{II} . The frequency modes depend on both differences of intrinsic frequency ($\omega_1 \sim \omega_2$) of the non-linear oscillator and linear coupling D . The behaviour of this type of system can be investigated when the beams are connected with two different driving sources which have independent frequency and amplitude. The displacement of the beams at or near the driving frequency depends on amplitude and phase. We can take specific values of the parameters relevant for the coupled nanomechanical resonator [100]: the mode frequency for the particular device is typically $\omega_1 = 2\pi \times 16.79 \text{ MHz}$ and $\omega_2 = 2\pi \times 17.25 \text{ MHz}$ the eigenvectors for coupled resonators are $\chi_I = (0.854, 0.521)$, $\chi_{II} = (-0.521, 0.854)$. We can find the frequency of individual resonators by inverting mode equations $\omega_1 = 2\pi \times 16.71 \text{ MHz}$ and $\omega_2 = 2\pi \times 16.92 \text{ MHz}$. The mode frequency separation is of the order of 200 KHz is consistent

with the tolerance of fabrication. The coupling strength is taken as $D = 2\pi \times 6.91 \text{ MHz}$. The response of the system for small dissipation and driving near the resonance condition can be calculated from Eq. (1.39) and Eq. (1.40) using perturbation approach [105]. In weak nonlinear regime, parametric coupled nonlinear oscillator is previously studied using secular perturbation theory [80, 106, 107]. Let us briefly, introduce the notation for slowly varying complex mode amplitudes A_1 and A_2 and driving force F_1 and F_2 where $x_j = \text{Re}[A_j e^{i\omega_j t}]$ near the resonant condition $F_j e^{i\Omega_j t} \approx \text{Re}[F_j e^{i\omega_j t}]$ (where j stand for 1 and 2). Substituting this in Eq. (1.39) and Eq. (1.40) we get reduced equation of motion as:

$$2i\omega_1 \dot{A}_1 + i\omega_1 \eta_1 A_1 + \beta_1 |A_1|^2 A_1 + \kappa_1 |A_2|^2 A_1 = F_1(t). \quad (1.41)$$

Similarly we can write it for A_2 . The coefficient of nonlinearity β_j and κ_j can be found by $\beta_{1,2}$ and eigenvectors $\chi_{1,2}$. We solve such a case in which each mode respond to drive frequency ω_{D_1} is set near the resonant frequency ω_1 where $A_1 \propto e^{i(\omega_{D_1} - \omega_1)t}$ with

$$|A_1|^2 = \frac{F_1^2}{[2\omega_1(\omega_{D_1} - \omega_1) - \beta_1 |A_1|^2 - \kappa_1 |A_2|^2]^2 + \eta_1^2 \omega_1^2}. \quad (1.42)$$

For single drive ($A_2 = F_2 = 0$), the cross-mode nonlinear coupling is not present κ_1 . The driving of one mode is used for tuning nonlinearity of second mode. This can be used to increase the dynamics range of oscillator by quenching the effective nonlinearity. This theory is useful for understanding, controlling and exploiting nonlinear behaviour of a coupled resonator.

The nonlinear nanomechanical oscillator get much attention in recent some year due to its abrupt change in dynamical behaviour depending on the parameters of the system. Chaos is widely observed behaviour in an nonlinear dynamical system. We are going to provide basic idea about chaos in the next section.

1.8 Chaos

For the last few years, the field of nonlinear dynamics seeks the attention of researchers [108, 109]. First study of nonlinear dynamics was done by Henri Poincare [110]. He figured out the whole set of variable required for the analytical solutions which is used to determine phase space and for a complete description of the state [111]. He observed in a three-body problem how a small perturbation can affect the solution [112]. To understand nonlinear dynamics he introduced the concept of phase space, Poincare section, periodic orbit, return map, bifurcation, fixed point, and so on. The first chaotic solution ever drawn is for Lorenz attractor [113]. Chaotic systems are unstable because they do not resist external disturbance but are navigated by them. Chaotic systems are deterministic because they can be solved with a few differential equations and make no reference to inherent change in the mechanism. Some systems are said to be chaotic if their evolution depends on the initial condition. In such cases with two different initial conditions, two different closed trajectories will be formed. Many natural systems are also said to be chaotic such as the solar system, brain and heart so on.

The main characteristic of a chaotic system is given by:

- System does not show a periodic behaviour.
- System will be sensitive to their initial condition.
- Chaotic motion is difficult to predict.
- If the system doing chaotic motion it will look random.
- For chaotic motion system will be nonlinear.

Chaotic motion is hard to predict and a lot of equations are required for computation. These systems are sensitive to their initial conditions, and a slight change in the initial conditions will lead to a different trajectory. This makes a chaotic system unpredictable.

1.8.1 Limitations of chaos theory

There are mainly two limitations: The first is due to relativity and the second is due to the uncertainty principle. It means within the laws of physics, it is impossible to simultaneously know everything because information must cross distances at a very slow rate. Second, is a fundamental principle of quantum mechanics stating that we can not simultaneously and precisely determine the position and momentum of subatomic particles. This is a fundamental property of the system, the more precisely we measure one the more we lose the other. The perfect example of chaos theory is weather, which we can not be predicted accurately. Control of chaos will give stabilization to the system which can be done by means of small perturbation. It will be a huge advantage if a chaotic motion is stable and predictable. If perturbation is small in comparison to the size of the system then it will not affect much on the natural dynamics of the system. There are several techniques to control chaos but two are most developed in this field (1) OGY method [114] and (2) Pyragas method [115]. Both methods require previous determination of unstable orbit to design controllable algorithms for chaotic systems. There are three ways to control the chaos.

- Changing its parameter so that range of fluctuation in the system can be limited.
- Applying a small perturbation to the system.
- Change the relationship between the system and the environment.

Chaos gives the realisation that even a simple system may perform complex dynamics. The difference between classical and quantum chaos is the phase trajectories in a classically chaotic system are very sensitive to the initial conditions while in a quantum case there are no phase trajectories but the chaos will manifest as Gaussian statistics of the energy spectrum. In quantum chaos, energy level statistics provide the information about the quantum systems if it follows Wigner statistics *i.e.*, level-repulsion is related to chaotic classical motion, while the lack of repulsion is related to the Poisson statistic and corresponds to

integrable motion. In a classically nonintegrable system, energy level repulsion will occur as shown by many numerical calculations. It is due to the interaction between unperturbed states which will lead to the formation of eigenstates which in the form of a superposition of unperturbed states.

In the next section we are going to expand our discussion about the quantum system interacting with their surrounding environment. Such type of system are said to be open quantum system.

1.9 Open quantum system

Most of the studies in general deal with a closed quantum system, that does not interact with the unwanted environment outside the world. A realistic system may interact with an unwanted environment. In quantum information processing, these unwanted interactions are shown as noise. What is the difference between open and closed systems? In a mechanical clock, a swinging pendulum will nearly be a closed system. When a pendulum interacts with the environment through friction, it will behave like an open system. However, for the dynamics of the pendulum one must take into account the damping effect, air friction and other imperfections of the pendulum. Similarly, the quantum systems are not perfectly closed for the desired operation when they are attached to external sources. The measurement on single quantum systems has been achieved in last few decades [116, 117]. This study will help in the applications related to quantum information processing [118, 119], quantum computation and ultrasensitive magnetometry. However, when there are uncontrolled interactions with the surroundings leading to decoherence of the quantum state, we will have a hurdle for realizing these technologies. The main challenge of this field is to protect the quantum state from decoherence due to the environment. High fidelity and dynamical decoupling can be exploited in the quantum system by reducing the environmental effect [120]. As we know from the Carnot cycle, the quantum system is isolated from the

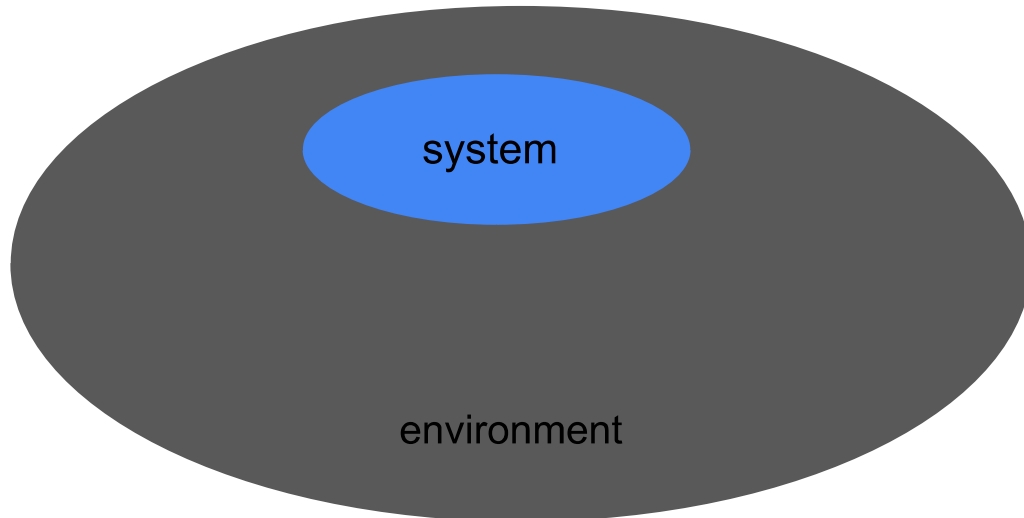


Fig. 1.7 (Color online) A total system divided into the system of interest, "System", and the environment.

environment. Some recent progress shows dynamical decoupling of a single spin system [121]. In this thesis, we mainly discuss the NV centre spin attached to the spin bath. NV centre spins can be optically imaged and show high coherence even at room temperature. These properties are used to gain a better understanding of spin decoherence [117, 122] as well as the basics of quantum information protocols even at room temperature [123, 124].

For the decoherence of NV centre spin, we investigate two different ways: In the first case, we study about the Markovian master equation while this is not the only process of decoherence of NV centre spin. The second case is due to the nuclear-spin bath surrounding NV centre spin. The information flow from the system to the environment is usually Markovian process while backflow of information is Non-Markovian process.

1.9.1 Markovian Lindblad Master Equation

First, we explore the dynamics of the system attached to a bath which is modelled as Markovian interaction. In this case dynamics of the quantum system are studied with the

help of the Lindblad equation [125, 126]. It plays important role in the field of quantum optics [127], condensed matter physics [128], quantum information and decoherence [129]. To investigate the time evolution of the reduced density matrix of a dissipating system, we first determine time evolution of total system and then trace out the environment degrees of freedom of the composite system. The density matrix of the composite system can be written as:

$$\rho_T = |\psi_T(t)\rangle\langle\psi_T(t)| = U^\dagger \rho(0)U, \quad (1.43)$$

where T represent total composite system consisting of the system and the environment and $U = \exp(-iHt)$ is a unitary operator. When we trace out the environment from total density matrix, we get density matrix of the system as:

$$\rho_S(t) = Tr_E(\rho_T(t)). \quad (1.44)$$

We can also study by considering von-Neumann equation for total density matrix of system as

$$\frac{\partial \rho_T(t)}{\partial t} = \frac{-i}{\hbar} [H, \rho_T(t)], \quad (1.45)$$

and after tracing out the environment, the evolution of density matrix will be given by

$$\frac{\partial \rho_S(t)}{\partial t} = \frac{-i}{\hbar} Tr_E([H, \rho_T(t)]). \quad (1.46)$$

Since we are not much interested in the dynamics of the environment unless it is required explicitly and the calculation for the full system usually consist of unnecessary details. For this purpose, we use the master equation approach to provide a reduction in computational effort in calculating over Eq. (1.44) and Eq. (1.46). The master equation leads to an approximate description of decoherence. Let us calculate the reduced density matrix from

a nonunitary evaluation. A master equation of reduced density matrix has the form

$$\frac{\partial \rho_S}{\partial t} = \mathcal{K}[\rho_S(t'), t' \leq t], \quad (1.47)$$

where \mathcal{K} is superoperator. For particular interest, Markovian master equation can be written as

$$\frac{\partial \rho_S}{\partial t} = \mathcal{L} \rho_S(t). \quad (1.48)$$

This equation is widely used in studying of decoherence. We will now use a dynamic map for discussion and their derivation and underlying assumptions.

1.9.2 Dynamical Map

We will take initially an uncorrelated total system such as system and environment $\rho_T(0) = \rho_S(0) \otimes \rho_E(0)$. Now, using Eq. (1.46) we will write the equation for state of the system as

$$\rho_S(0) \rightarrow \rho_S(t) = \mathcal{Y}_t \rho_S(0), \quad (1.49)$$

with $\mathcal{Y}_t \rho_S(0) = \text{Tr}_E \{ U(t) [\rho_S(0) \otimes \rho_E(0)] U^\dagger(t) \}$, \mathcal{Y}_t in Eq. (1.48) and Eq. (1.49) represents a dynamical map. This will map an initial quantum state $\rho(0)$ to a final quantum state $\rho(t)$ at time t . This equations will obey quantum rules. The above can also be written using Karus operator $\mathcal{K}_n(t)$ as

$$\mathcal{Y}_t \rho_T = \sum_n \mathcal{K}_n(t) \rho_S(0) \mathcal{K}_n^\dagger(t), \quad (1.50)$$

where $\mathcal{K}_n(t)$ is operator in Hilbert space H_S . Eq. (1.49) represents how the state of an open quantum system changes in time. The dynamical map will follow these three mathematical conditions [130, 131] as below:

1. **Complete positivity-** The eigenvalues of the density operator must be positive as they are the physical interpretation of probabilities. Density operator must be positive semi-definite operator. Complete positivity is must required condition [125, 126, 130, 131, 132]. Extension $\mathcal{Y}_t \otimes id_n$ of \mathcal{Y}_t to a composite Hilbert space $H_{ext} = H_S \otimes \bar{H}_n \equiv H_S \otimes \mathbf{C}^n$, $\mathcal{Y}_t \otimes id_n$ where id_n is identity of Hilbert space \bar{H}_n . The motivation behind this is that if we take an ancillary system A which is assumed to have no intrinsic dynamics *i.e.*, $H_A = 0$ and placed it at a large distance from the system of interests such that it will not interact with the system of interest S , then the dynamical map related to the composite system SA is given by $\mathcal{Y}_t \otimes id_n$ and it will be positive for any state of composite system. If this condition is not satisfied then S and A start out of entanglement means that the quantum correlations between S and A come from some past interaction prior to the initial time and the dynamical map $\mathcal{Y}_t \otimes id_n$ will provide a negative probability. It means that in a complete positivity case \mathcal{Y}_t will generate consistent dynamics even when the system S was initially correlated with another system.

2. **Convex linearity-** Convex linear combination of density operators can be represented as $\rho = \eta\rho_1 + (1 - \eta)\rho_2$ with $0 \leq \eta \leq 1$. This will represent the mixture of two ensemble ρ_1 and ρ_2 with probabilities η and $(1 - \eta)$. Thus it is required for time evolved mixture again to evolve individually under dynamical map:

$$\mathcal{Y}_t\rho = \mathcal{Y}_t\{\eta\rho_1 + (1 - \eta)\rho_2\}. \quad (1.51)$$

3. **Trace preservation-** A time evolved density matrix will always have trace one, *i.e.*,

$$Tr\{\mathcal{Y}_t\rho\} = 1 \quad (1.52)$$

We emphasize the characteristic of dynamical maps in terms of completely positive, convex linear and trace-preserving.

1.9.3 Non-Markovian Behavior of Quantum Processes in Open Systems

We have already mentioned that decoherence in the NV centre is not only due to the Markovian master equation. It may also be due to the nuclear spin bath of C nuclei around NV center in diamond. In the last few years, theoretical study of non-Markovian systems is increased because of different analytical methods and numerical techniques that have been developed (see, for example, Refs. [133, 134, 135, 136]). The main question needing for explanations are: How quantum non-Markovianity can be defined and how to quantify the degree of non-Markovianity? For answering these questions one can measure the non-Markovianity of an open quantum system which in mathematical terms is a dynamical map of a time evolved state. Here, we develop a measure for non-Markovianity. It depends on the trace distance of two quantum states which also describes the probability of distinguishing these states. In a Markovian process, the distinguishability between any two states reduces while in the non-Markovian process it increases. The loss of distinguishability of states can also be stated as a flow of information from an open system to the environment while a key feature of the non-Markovian process is the reverse flow of information from the environment to the open system. To measure non-Markovianity [137], we calculate trace of the distance between two quantum states ρ_1 and ρ_2 which is defined as

$$\mathbf{D}(\rho_1, \rho_2) = \frac{1}{2} |\rho_1 - \rho_2|, \quad (1.53)$$

where $|A| = \sqrt{A^\dagger A}$ and \mathbf{D} must satisfy $0 \leq \mathbf{D} \leq 1$. It will give a clear interpretation of the distinguishability of states. Let Alice prepares two quantum states in ρ_1 and ρ_2 each

having probability $\frac{1}{2}$, Now she gives the system to Bob who will do some measurements to predict whether the system was in state ρ_1 or ρ_2 . The quantity $\frac{1}{2}[1 + \mathbf{D}(\rho_1, \rho_2)]$ is then equal to the probability that Bob will identify the state of the system. Thus, trace distance is a measure of distinguishability of the states. Another feature of trace distance is given that complete positive and trace-preserving (CPT) maps φ is a contraction for this metric [138]

$$\mathbf{D}(\varphi\rho_1, \varphi\rho_2) \leq \mathbf{D}(\rho_1, \rho_2). \quad (1.54)$$

It means that the distinguishability of states will never increase in no trace-preserving operations. We introduce a quantum process which follows Markovian master equation

$$\frac{d\rho}{dt} = \mathcal{L}\rho(t), \quad (1.55)$$

where

$$\mathcal{L}\rho = -i[H, \rho] + \sum_k \gamma_k \{B_k \rho B_k^\dagger - \frac{1}{2} \{B_k^\dagger B_k, \rho\}\}. \quad (1.56)$$

The Hamiltonian H and Lindblad operator B_k both are time independent and γ is a positive dephasing parameter. It will leads to completely positive and trace-preserving map $\varphi(t) = \exp(\mathcal{L}t)$ so that density matrix will become $\rho(t) = \varphi(t)\rho(0)$. By semi-group property $\varphi(\tau+t) = \varphi(\tau)\varphi(t)$ Eq. (1.54) can be written as

$$\mathbf{D}(\rho_1(\tau+t), \rho_2(\tau+t)) \leq \mathbf{D}(\rho_1, \rho_2), \quad (1.57)$$

where, $\rho_{1,2}(t) = \varphi(t)\rho_{1,2}(0)$. For any fixed pair of initial state $\rho_{1,2}(0)$ the trace distance of the state $\rho_{1,2}(t)$ will decrease in time for all quantum dynamical semigroup $\varphi(t)$. This implies that in the Markovian process the state becomes less distinguishable and it is interpreted as a loss of distinguishability in the flow of information from the system to the

environment. Let us take master equation with time dependent operator

$$\frac{d\rho(t)}{dt} = \mathcal{F}(t)\rho(t). \quad (1.58)$$

To preserve the Hermiticity and trace of the density matrix we can write time dependent operator in the form

$$\mathcal{F}(t)\rho = -i[H(t), \rho] + \sum_k \gamma_k(t) \{B_k(t)\rho B_k^\dagger(t) - \frac{1}{2}\{B_k^\dagger(t)B_k(t), \rho\}\}, \quad (1.59)$$

where $H(t)$ is time-dependent Hamiltonian and $B_k(t)$ time-dependent Lindblad operator and $\gamma_k(t)$ is time-dependent dephasing parameter. For time-dependent dynamical map $\varphi(t_2, t_1)$ can be written as

$$\varphi(t_2, t_1) = T \exp \left[\int_{t_2}^{t_1} dt' \mathcal{F}(t') \right]. \quad (1.60)$$

This will transform initial state to state at time t .

$$\varphi(t) = \varphi(t, 0). \quad (1.61)$$

The dynamical map has divisibility property, the CPT map of $\varphi(\tau + t, 0)$ can be written as a composition of

$$\varphi(\tau + t, 0) = \varphi(\tau + t, t) \varphi(t, 0). \quad (1.62)$$

Dynamical semigroups have property $\varphi(t_2, t_1) = \varphi(t_2 - t_1)$ then, we can write $\varphi(\tau + t) = \varphi(\tau) \varphi(t)$. We show that Eq. (1.57) hold for all the time dependent Markovian master equations. We define rate of trace distance as:

$$\eta(t, \rho_{1,2}(0)) = \frac{d}{dt} D(\rho_1(t), \rho_2(t)). \quad (1.63)$$

For $\eta(t, \rho_{1,2}(0)) \leq 0$ the process is Markovian and when $\eta(t, \rho_{1,2}(0)) \geq 0$, the process is said to be non-Markovian. We interpreted the non-Markovian process as the backflow of information from the environment to the system. Therefore, in this case system may not thermalize for a long time. How one can measure non-Markovianity? A good measure of non-Markovianity will be the increase in distinguishability between the states in whole time range *i.e.*, the backflow of information from the environment to the system. Non-Markovianity can be measured through the relation

$$\mathcal{N}(\varphi) = \max_{\rho_{1,2}(0)} \int_{\eta>0} dt \eta(t, \rho_{1,2}(0)). \quad (1.64)$$

Time-integration represented in Eq. (1.64) can take value from time interval range (a_k, b_k) in which $\eta(t, \rho_{1,2}(0))$ is positive and maximum is taken over all pairs of initial states [139].

We can also present Eq. (1.64) in the form

$$\mathcal{N}(\varphi) = \max_{\rho_{1,2}(0)} \sum_k [D(\rho_1(b_k), \rho_2(b_k)) - D(\rho_1(a_k), \rho_2(a_k))]. \quad (1.65)$$

For calculating this quantity one can measure trace distance over time interval (a_k, b_k) for any pair of initial states and then sum up for all the intervals. Then $\mathcal{N}(\varphi)$ can be obtain from determining the maximum over all the pairs of initial states.

We studied about the decoherence due to the influence of environment in this section and we are going to expand our discussion about entanglement in the next section.

1.10 Entanglement

Entanglement is a pure quantum phenomenon in which a group of quantum particles shares non classical correlation and the state of each particle in a composite system can not be described independently [140]. An entangled system can be described as one whose states can not be separable from its local constituents. Entanglement in the many-body

systems gives an understanding of quantum phase transition and various phases of many-body systems. When the system is composed of more than two subsystems *i.e.*, quantum correlation exist between them, they are Multipartite entangled. Multipartite entanglement is already studied in past [141] it is an important source for understanding the field of quantum computation and information using quantum many body system. One of the quantifiers of multipartite entanglement is the geometric measure of entanglement which does not explicitly consider subsystems and measures the overall entanglement in the system [142]. But it fails to give information about the number of parties involved in the entanglement. Other measure known as quantum Fisher information, gives information about the number of parties involved in the entanglement [143]. We can begin discussing the entanglement for the simplest case which is the entanglement of the pure state. Consider any general quantum system containing two parts labelled as A and B . Any pure state $|\Psi\rangle$ can be written as

$$|\Psi\rangle = \sum_i^N v_i |\psi_i^A\rangle \otimes |\psi_i^B\rangle, \quad (1.66)$$

where $|\psi_1^A\rangle, \dots, |\psi_N^A\rangle$ and $|\psi_1^B\rangle, \dots, |\psi_N^B\rangle$ are orthogonal states of subsystems A and B and v_i is a constant. Let the total system can be defined by the state $\rho = |\Psi\rangle\langle\Psi|$, then reduced density matrix of a subsystem is defined by taking partial trace as

$$\rho_A = Tr_B(\rho). \quad (1.67)$$

The entanglement entropy is given by

$$S_A = -Tr[\rho_A \log_2 \rho_A]. \quad (1.68)$$

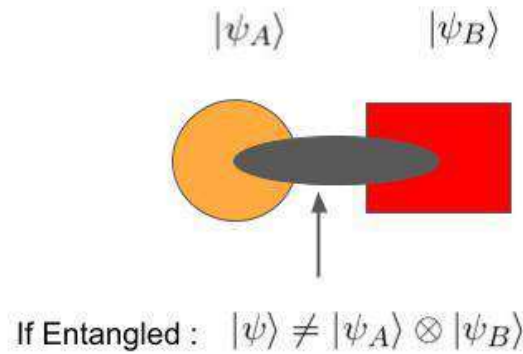


Fig. 1.8 Schematics representation of Entanglement.

It can also be written in the form

$$S = - \sum_k^N c_k^2 \log_2 c_k^2. \quad (1.69)$$

This quantity is also known as von-Neumann entropy associated with the density matrix of either of the two subsystems. Here c_k^2 s are the eigenvalues of the density matrix.

According to quantum mechanics, the total Hilbert space of a system is a tensor product of the subsystem spaces. The total state of a system can be written as

$$|\psi\rangle = \sum_{i_1, \dots, i_n} A_{i_1 \dots i_n} |i_1\rangle \otimes \dots \otimes |i_n\rangle. \quad (1.70)$$

It can not be described as a product of the state of individual subsystems

$$|\psi\rangle \neq |\psi\rangle_1 \otimes |\psi\rangle_2 \otimes |\psi\rangle_3 \otimes \dots \otimes |\psi\rangle_N. \quad (1.71)$$

It is impossible to assign a single state vector to any one of the N subsystems. Therefore, the subsystems are entangled is also shown in Fig. 1.8. In a quantum system, entanglement is a striking feature and is key to realising many quantum physical phenomena such as quantum information, quantum teleportation, and quantum computation [144], which cannot be accounted by classical physics. For quantitative measurement of entanglement of

two qubit, we can use concurrence [145], which was first analytically derived by Wootters [146]. Some study shows concurrence plays an essential role in describing quantum phase transition [147, 148] in quantum many-body systems. Let's take a generalized definition of concurrence for a pure state $|\phi\rangle$ which is a tensor product of two finite dimension Hilbert state H_A and H_B for two subsystems. The concurrence is defined as:

$$C(|\phi\rangle) = \sqrt{2(1 - \text{Tr}(\rho_A^2))} \quad (1.72)$$

Where ρ_A is the reduced density matrix of subsystem A after tracing out B . The concurrence for two qubit mixed state ρ can be written as:

$$C(\rho) = \text{Max}\{0, \lambda_1 - \lambda_2 - \lambda_3 - \lambda_4\}, \quad (1.73)$$

Where λ_i 's are the square-root eigenvalue of $\rho\bar{\rho}$ in decreasing order. Here $\bar{\rho}$ is defined in terms of spin-flip operator:

$$\bar{\rho} = (\sigma_y \otimes \sigma_y)\rho^*(\sigma_y \otimes \sigma_y), \quad (1.74)$$

where ρ^* is conjugate of density matrix and σ_y is Pauli matrix.

In this section we explored about quantum entanglement. Next, we explore about quantum information scrambling which quantifies that how a quantum information localized initially in a quantum many body system spreads in time.

1.11 Scrambling in a quantum system

The thermalization of an isolated quantum system is the main challenge [149, 150]. The thermalisation of a quantum system was studied at various time scales, from early time scrambling to intermediate time and saturation time. Scrambling describes the spreading

of quantum information to all degrees of freedom of the system. To study scrambling in a quantum systems we need to study the growth of commutators of local operators which is also related to the physics of classical chaos and do an analysis of the butterfly effect whereas local perturbation will spread over the entire system [151]. We can get scrambling time from the decay of an out-of-time-order correlation (OTOC) function.

$$\mathcal{F}(t) = \langle W(t)VW(t)V \rangle. \quad (1.75)$$

Here, W and V are two local commuting unitary operators. For studying this we consider two local operator W and V and their unitary time evolution under the Hamiltonian is defined as $W(t) = \exp(iHt)W \exp(-iHt)$. The correlating function \mathcal{F} is defined in terms of two wave functions which are time evolved in different manner. For many body systems $\mathcal{F}(t)$ tells us about the spread of quantum information by measuring how swiftly the interaction causes two local commuting operators to fail to commute which can be defined as

$$C(t) = \frac{1}{2} \langle [\hat{W}(t), V]^\dagger [\hat{W}(t), V] \rangle, \quad (1.76)$$

Where $W(t)$ is a Heisenberg operator and if W and V are Pauli observable. Since, Pauli observables are unitary and hermitian then $C(t)$ can also be written as

$$C(t) = 1 - Re[\mathcal{F}(t)]. \quad (1.77)$$

Here $\langle . \rangle$ is specified as quantum mechanical average with ground state or thermal average taken over Gibbs's state at finite temperature.

1.12 Outline of the Thesis

Chapter 2 discusses about coupling of mathematical pendulum to NV center electron spin. Exact analytical solution is accessible in spite of nonlinearity in the system. We study the combined effect of coupling and driving between the spin and mathematical pendulum. The work presented in this chapter is derived from the original work published as "Generation of coherence in an exactly solvable nonlinear nanomechanical system" by A. K. Singh *et. al.* Phys. Rev. B 101, 104311, (2020).

In Chapter 3 we discuss about hybrid quantum-classical system. Which consist of a NV center electron spin (quantum spin) coupled to a nanocantilever (classical). In this chapter we see the effect of classical cantilever onto the quantum spin. The work presented in this chapter is derived from the original work accepted for publication as "Hybrid quantum-classical chaotic NEMS" by A. K. Singh *et. al.* Physica D: Nonlinear Phenomena (2022).

In Chapter 4 we discuss about a model of two nonomechanical oscillator coupled to two NV center electron spin. Where NV center electron spin are not directly coupled while oscillators are directly coupled with each other. The correlation between NV spin arises due to feedback exerted by NV center electron spin to first oscillator and transferred from the first oscillator to the second oscillator via the direct coupling. The work presented in this chapter is derived from the original work published as "Scrambling and quantum feedback in a nanomechanical system" by A. K. Singh *et. al.* Eur. Phys. J. D 76, 1 (2022).

In Chapter 5 we present summary and scientific conclusions derived from various works conducted during the Phd program. The future plan is also discussed briefly.